Preprints of the 9th Vienna International Conference on Mathematical Modelling
Vienna, Austria, February 21-23, 2018

Experimental validation and comparison of time-optimal and industrial strategy for membrane separation process

Ayush Sharma, Richard Valo, Martin Kalúz, Radoslav Paulen, Miroslav Fikar

Slovak University of Technology in Bratislava, Slovakia, (e-mail: {ayush.sharma, richard.valo, martin.kaluz, radoslav.paulen, miroslav.fikar}@stuba.sk).

Abstract: In this paper, a time-optimal strategy is implemented for batch membrane separation of lactose-salt solution. Parameters of the flow-rate model are estimated by solving a dynamic optimization problem that minimizes the difference between experimental and simulated system outputs. The estimated flow-rate models are used to formulate an optimal control problem (OCP) which minimizes the batch time using diluant addition rate as the control input. This time-optimal strategy is found analytically and is validated using experiments, where lactose is concentrated and concentration of salt is reduced. The processing time is compared with classical industrial strategy to emphasize on the outcomes.

Keywords: Membrane separation, Parameter estimation, Time-optimal control, Non-linear optimization, Pontryagin's minimum principle.

1. INTRODUCTION

Membranes in industry separate, concentrate, remove impurities, and clarify solutions. They are an important part of food, chemical, and biotechnology industries. Based on the component size and operating parameters, the membrane separation processes are divided into micro- (MF), ultra- (UF), nanofiltration (NF) and reverse osmosis. NF retains molecules with molecular mass of 200–1,000 g/mol. The applied pressure range for NF is 3–50 bar (Artuğ, 2007).

NF applications include water softening, waste-water treatment, vegetable oil processing, beverage, dairy (Chen et al., 2017), juice and sugar industry (Salehi, 2014; Conidi et al., 2017). In production of lactose from cheese whey, NF concentrates lactose molecules while passing salts (Das et al., 2016). This concentrated lactose is a commonly used material in the pharmaceutical industry as a carrier of drugs, e.g., in inhalations for asthma patients (Boerefijn et al., 1998). Besides pharmaceutical industry, in food and beverage industry lactose is emerging widely as a source for epilactose, galacto-oligosaccharides (Verasztó et al., 2013; Cohen et al., 2017), lactitol, lactobionic acid, and other important lactose derivatives (Gutiérrez et al., 2012).

Diafiltration (DF) is a technique that uses MF, UF, and NF to lower the concentration of impurities with the help of a diluant. In combination with NF, DF is applied to lower the concentration of salts (Yin et al., 2011). This combination of NF and DF, i.e. nanodiafiltration, abbreviated as NDF by Chandrapala et al. (2016) (NDF is used further in this paper) is also used for removal of lactic acid from acid dairy whey, for better crystallization of lactose. Time-optimal operation to concentrate lactose and remove salt using NDF, is the objective of this study.

The model that relates the membrane permeation rate and solute concentrations holds utmost importance in order to implement the time-optimal strategy. Modeling of permeate flow based on solute concentrations for membrane processes has been dealt before in the literature; e.g. Jaffrin and Charrier (1994) fitted permeate flux as an inverse polynomial function of albumin and ethanol concentrations and van den Berg and Smolders (1990) researched on various resistance, gel-polarization, and osmotic pressure models. All these and most of the other modeling works done in past are for UF, and not much of research has been done in modeling the permeation of NDF. Regarding time-optimal control of membrane separation processes, only simulation studies (Fikar et al., 2010; Jelemenský et al., 2015) using the existing models have been done.

In our recent study (Sharma et al., 2016), existing flux/permeation models with fouling from Hermia (1982) were fitted to experimentally obtained data for the studied solution, but the model included only lactose concentration. In Sharma et al. (2017), fitting of models from literature and a novel model as a function of both concentrations was done. The fitting approach was static and the optimal operation shown in simulation studies.

This paper describes dynamic fitting of permeate flow over the solution components (lactose and NaCl), by optimally estimating the parameters of models from literature. These models are used to design optimal operation strategy to minimize processing time, using Pontryagin's minimum principle. Finally, this time-optimal operation is implemented on a pilot-scale plant for validation and is compared with classical industrial strategy. The NDF

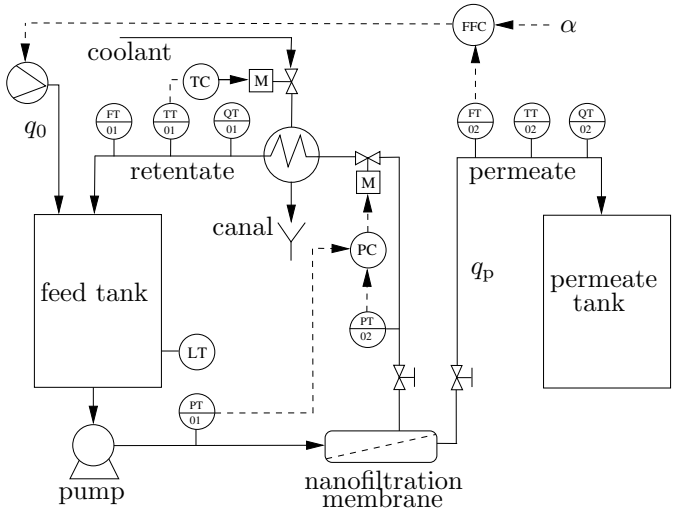

Fig. 1. Nanodiafiltration process scheme.

experiments are done to concentrate lactose (product), and to reduce the concentration of NaCl (impurity). This implementation of time-optimal membrane operation and its comparison with classical industrial approach is the prime novelty of this research.

2. PROCESS DESCRIPTION

2.1 Materials

Lactose monohydrate (M = 360.31 g/mol) and sodium chloride (M = 58.44 g/mol) manufactured by Centralchem (Slovakia) were used as solutes and reverse osmosis water was used as a solvent to prepare solutions. The plant has an NFW-1812F nanofilter membrane manufactured by Synder Filtration, USA, with a cut-off range 300–500 Da, and a membrane area of $A = 0.465\,\mathrm{m}^2$.

2.2 Plant Description & Methods

The scheme of the plant is shown in Fig. 1. The batch starts with adding initial feed volume (V_0) to the feed tank comprising initial concentrations of lactose and NaCl ($c_{1,0}, c_{2,0}$). The pump at certain trans-membrane pressure forces the feed towards the membrane in cross-flow mode, where the solution separates into two streams. The concentrated/rejected one is called retentate and it comprises lactose and NaCl. The stream passing through the membrane is called permeate, and it contains NaCl. The permeate flow rate is measured in L/h using sensor FT02.

The concentration of NaCl (c_2) in the retentate is inferred from the conductivity measurements (sensor QT01) using the experimentally obtained linear model

$$c_2\,[\mathrm{g/L}] = 0.0007 \times \mathrm{QT}\,[\mu\mathrm{S/cm}] - 0.6949. \tag{1}$$

Lactose concentration (c_1) is inferred from the mass balance in the feed tank using the level measurement (sensor LT). This is described in the next section. The trans-membrane pressure (TMP) defined as,

$$\mathrm{TMP} = \frac{P_{\mathrm{feed}} + P_{\mathrm{retentate}}}{2} - P_{\mathrm{permeate}} = 20\,\mathrm{bar}, \tag{2}$$

is controlled at a constant value during the experiment. This control is achieved using a pressure controller (PC). The pressure could be changed by two actuators, i.e., the pump and the retentate side valve. To protect the pump and keep it at a constant rotational speed, the retentate valve opening is used as the manipulated input. The temperature of the solution is maintained around a constant value of 27 °C using a heat exchanger and a temperature controller (TC). Due to imperfection of the employed valve, the temperature cannot be held constant and has variance of ±1 °C. This causes fluctuations in permeate flow and in induced concentration measurements.

The diluant (water) addition for NDF is done using another pump. The dilution rate is the input variable for NDF process and it is defined as

$$\alpha = q_0/q_{\mathrm{p}}, \tag{3}$$

where q_0 and q_{p} denote the inflow of the diluant into the feed tank and permeate outflow, respectively.

The classical control of batch DF mostly uses piece-wise constant α using three simple modes (Jaffrin and Charrier, 1994; Foley, 2006), i.e.

- No diluant input ($\alpha = 0$), i.e. concentration mode (C): in this mode, due to no diluant inflow, the volume decreases. As a result, the concentration of lactose increases, while the concentration of NaCl stays constant.
- The diluant inflow equals the outflow of permeate ($\alpha = 1$), i.e. constant volume diafiltration mode (CVD): lactose concentration remains constant while NaCl concentration decreases in this mode.
- Diluant flow rate is less than the outflow of permeate ($0 < \alpha < 1$), i.e. variable volume diafiltration mode (VVD): volume decreases in this mode, and hence lactose concentration increases, while due to the dilution of solution, NaCl concentration decreases.

In addition, Lutz (2015); Paulen and Fikar (2016) have proposed two new basic modes:

- Dynamic volume diafiltration (DVD): this is similar to VVD mode, but unlike VVD α is not a constant but is varying with time ($0 < \alpha(t) < 1$).
- Pure dilution mode (D): a certain amount of diluant is instantaneously added to the solution. This can be symbolically represented by $\alpha = \infty$. Both lactose and NaCl concentrations decrease in pure dilution mode.

2.3 Process Model

The standard DF model with two solutes can be described by three differential equations (Paulen and Fikar, 2016)

$$\frac{\mathrm{d}c_1}{\mathrm{d}t} = \frac{c_1 q_{\mathrm{p}}}{V}(R_1 - \alpha), \qquad c_1(0) = c_{1,0}, \tag{4a}$$

$$\frac{\mathrm{d}c_2}{\mathrm{d}t} = \frac{c_2 q_{\mathrm{p}}}{V}(R_2 - \alpha), \qquad c_2(0) = c_{2,0}, \tag{4b}$$

$$\frac{\mathrm{d}V}{\mathrm{d}t} = (\alpha - 1)q_{\mathrm{p}}, \qquad V(0) = V_0, \tag{4c}$$

where V is the actual volume in the feed tank and the constants R_1, R_2 are rejection coefficients of the respective solutes. These are dimensionless numbers in the interval $[0, 1]$. $R_i = 0$ implies that the ith solute passes through the membrane without any resistance. On the contrary, $R_i = 1$ means that the membrane blocks the solute completely and its concentration in the permeate is zero.

NF membrane blocks lactose completely, hence $R_1 = 1$. This is in compliance with the data from the membrane producer (Synder, 2014). The value $R_1 = 1$ therefore implies that the amount/mass of lactose in the system (for our batch process) remains constant, and its concentration can be inferred from the actual volume using;

$$c_1 V = c_{1,0} V_0 \quad \Rightarrow \quad c_1 = \frac{c_{1,0} V_0}{V}. \tag{5}$$

2.4 Permeate Flow Modeling and Parameter Estimation from Experimental Data

Based on experiments and on our previous results (Sharma et al., 2016, 2017) it is clear that at constant temperature and TMP; NF permeation rate depends on concentrations of both lactose and NaCl, i.e. $q_\mathrm{p} = q_\mathrm{p}(c_1, c_2)$. The membrane fouling occurs only for a short initial period and stabilizes quickly. The lactose molecules being larger in size have significantly larger effect on the permeate flow when compared to NaCl molecules. Data from an NDF experiment that concentrated lactose from 40 g/L to 120 g/L, (C mode) and that reduced NaCl from 3.35 g/L to 1 g/L (CVD mode) was used to perform the fitting of models from literature of such kind. The experiment was done in total recirculation mode (permeate returns to feed tank, volume and concentrations remain constant) until fouling got constant, and then permeate was allowed to leave the system. 56 data points of flow rate were used to perform model fitting. The sample time was 0.025 h.

Two different models were fitted with the permeate flow rate data i.e., a function of lactose and NaCl concentration:

- Limiting flux (LF) model: This model has been taken from Tang and Leckie (2007); Blatt et al. (1970). The model defines the permeate flow rate as a function of time-varying lactose (macro-solute) concentration and the parameters, i.e. mass transfer coefficient (γ_1) and limiting concentration of lactose (γ_2).

  $$q_\mathrm{p} = \gamma_1 \ln\left(\frac{\gamma_2}{c_1}\right) = \gamma_1 \left(\ln \gamma_2 - \ln c_1\right). \tag{6}$$

  This model is used as the dependence of permeate flow on NaCl concentration is quite low. This can be inferred from studying the CVD part of experiment (Fig. 2), where the NaCl is decreasing, but the magnitude of change in q_p is very small.

  Two such models have been fitted. Firstly, by taking the complete experimental data (both C and CVD modes), i.e. LF_1. Secondly, as this model is only a function of c_1, and c_1 is not varying a lot during the second part of experiment (CVD mode in Fig. 3), hence a model was fitted using only the data from the first part of experiment, i.e. LF_2.
- Generalized limiting flux (GLF) model: This model has been taken from Rajagopalan and Cheryan (1991) and is defined as

  $$q_\mathrm{p} = \ln\left(\frac{\gamma_2}{c_1 c_2^{\gamma_3}}\right)^{\gamma_1} = \gamma_1 \left(\ln(\gamma_2) - \ln(c_1) - \gamma_3 \ln(c_2)\right). \tag{7}$$

  It incorporates concentrations of both solutes and can be reduced to the limiting flux model with $\gamma_3 = 0$.

The optimal parameter estimation problem to fit the flow rate data to the above models and the concentration data to state values can be formulated as:

$$\min_{\gamma_1,\gamma_2,\gamma_3} \ \frac{(q_\mathrm{p} - q_\mathrm{p,m})^2}{\delta_1} + \frac{(c_1 - c_\mathrm{1,m})^2}{\delta_2} + \frac{(c_2 - c_\mathrm{2,m})^2}{\delta_3} \tag{8a}$$

s.t.

$$\dot{c}_1 = c_1^2 \frac{q_\mathrm{p}}{c_{1,0} V_0}(R_1 - \alpha), \tag{8b}$$

$$\dot{c}_2 = c_1 c_2 \frac{q_\mathrm{p}}{c_{1,0} V_0}(R_2 - \alpha), \tag{8c}$$

$$c_1(0) = c_{1,0}, \quad c_2(0) = c_{2,0}, \tag{8d}$$

$$c_1(t_\mathrm{f}) = c_\mathrm{1,f}, \quad c_2(t_\mathrm{f}) = c_\mathrm{2,f}, \tag{8e}$$

$$q_\mathrm{p} = (6) \text{ or } (7), \tag{8f}$$

with the given profile of $\alpha(t)$. The experimental flow rate and states are represented by $q_\mathrm{p,m}$ and $c_\mathrm{1,m}$, $c_\mathrm{2,m}$ respectively. The weighing of each term in the objective is represented by coefficients, δ_1, δ_2, and δ_3, which are set to experimentally observed variances of corresponding measurements. The above non-linear least-squares problem was implemented and solved using MATLAB, and the states were integrated using an ode45 solver. The resulting parameters are given in Table 1 and the permeate flow rates and concentrations in Figs. 2–4. It can be observed that the GLF model fits the data better than the LF models, especially in the second part of the experiment with $\alpha = 1$. This is expected as the GLF model can accommodate the variations in the concentration $c_2(t)$. The value of sum of squared errors was at the minimum for GLF model, increased slightly for LF_1 model, and was maximum for LF_2 model. The comparison of the estimation between LF_1 and LF_2 models shows that for C mode the LF_2 model fits the data better, but when simulated for CVD mode the results were worst. It concretes that even though LF model is solely a function of c_1, still data for both C and CVD modes are required for fitting the complete NDF data. The measured and the simulated concentrations were satisfactorily corresponding to each other, for all fitted models (Fig 3, 4).

Table 1. Parameters of the models.

model	GLF	LF_1	LF_2
γ_1	3.0	2.8	3.4
γ_2	1109.9	1246.7	723.7
γ_3	0.1	-	-

3. PROCESS OPTIMIZATION

The objective is to find a time-dependent input function $\alpha(t)$, which guarantees the transition from the given initial $c_{1,0}, c_{2,0}$ to final $c_\mathrm{1,f}, c_\mathrm{2,f}$ concentrations in minimum time. This time-optimal problem can be formulated as:

$$\mathcal{J}^* = \min_{\alpha(t)\in[0,\infty)} \int_0^{t_\mathrm{f}} 1 \,\mathrm{d}t \tag{9a}$$

s.t.

$$\dot{c}_1 = c_1^2 \frac{q_\mathrm{p}}{c_{1,0} V_0}(R_1 - \alpha), \qquad c_1(0) = c_{1,0}, \tag{9b}$$

$$\dot{c}_2 = c_1 c_2 \frac{q_\mathrm{p}}{c_{1,0} V_0}(R_2 - \alpha), \qquad c_2(0) = c_{2,0}, \tag{9c}$$

$$c_1(t_\mathrm{f}) = c_\mathrm{1,f}, \quad c_2(t_\mathrm{f}) = c_\mathrm{2,f}, \tag{9d}$$

$$\text{Eq. (6) or (7).} \tag{9e}$$

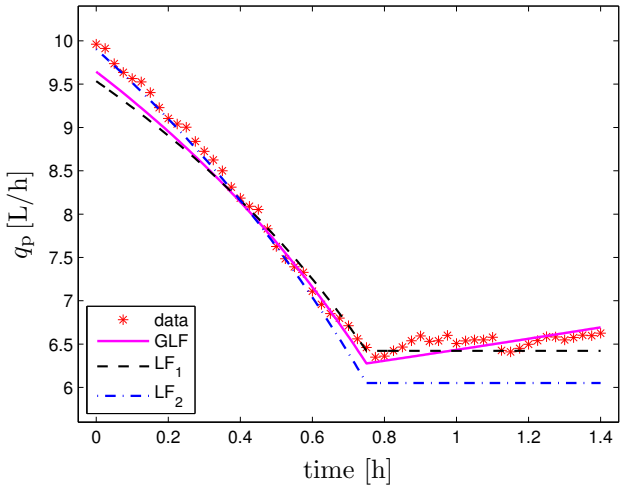

Fig. 2. Permeate flow rate measurements vs simulated estimated models.

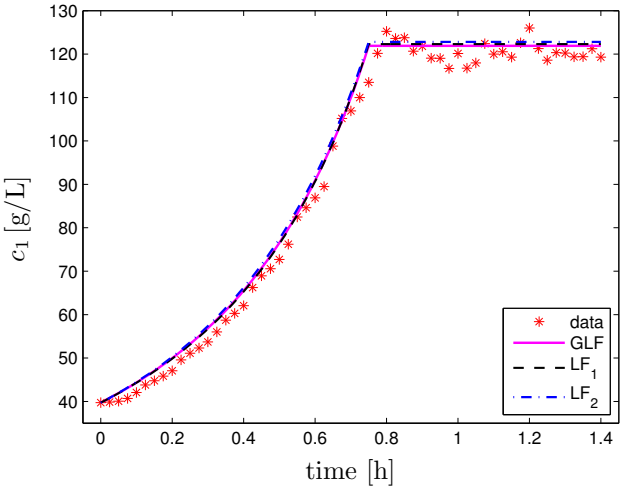

Fig. 3. Comparison of lactose concentration: measured vs simulated data based on estimated models.

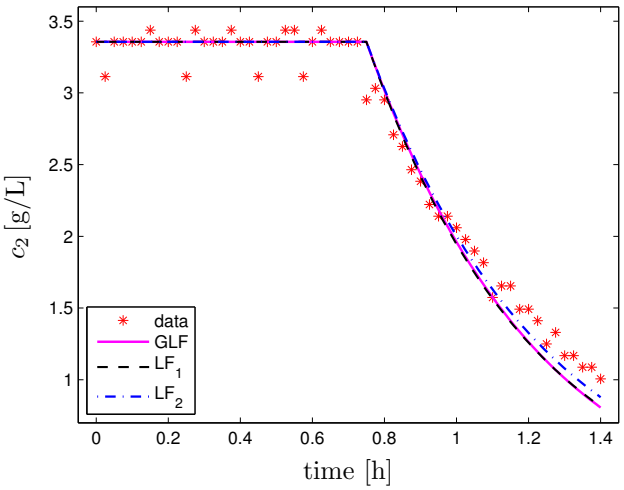

Fig. 4. Comparison of NaCl concentration: measured and simulated data based on estimated models.

As the LF_2 model was not very efficient in tracking the experimental data from the CVD part of the experiment, hence it has been excluded from the optimization study, and only GLF and LF_1 models are used.

The analytical approach towards finding an input strategy that minimizes the batch time of the diafiltration process is taken from Paulen and Fikar (2016). This approach is based on Pontryagin's minimum principle (Pontryagin et al., 1962). The optimal strategy can be described as a switching non-linear feedback control that consists of three arcs. The first and the third one are on the input boundaries, while the middle one is a sensitivity arc derived from the singular control. This singular/sensitivity arc can in general be represented as

$$S = q_\mathrm{p} + \frac{\partial q_\mathrm{p}}{\partial c_1} c_1 + \frac{\partial q_\mathrm{p}}{\partial c_2} c_2 = 0. \tag{10}$$

The equation $S = 0$ marks the switching condition from minimum/maximum input to the input implemented during the singular arc, i.e.

$$\alpha_s = \frac{\frac{\partial S}{\partial c_1} c_1}{\frac{\partial S}{\partial c_1} c_1 + \frac{\partial S}{\partial c_2} c_2}. \tag{11}$$

The resulting S and α_s for both GLF and LF_1 models can be formulated as,

(1) *GLF model*:

$$S = q_\mathrm{p} - \gamma_1 (\gamma_3 + 1) = 0, \tag{12}$$

$$\alpha_s = \frac{1}{1 + \gamma_3} = 0.91. \tag{13}$$

(2) *LF_1 model*:

$$S = q_\mathrm{p} - \gamma_1 = 0, \tag{14}$$

$$c_1^* = \gamma_2 / \mathrm{e}, \tag{15}$$

$$\alpha_s = 1. \tag{16}$$

Here c_1^* stands for the switching concentration of lactose, and can be derived from (14). As discussed above, these three-step optimal strategies consists of control arcs on the admissible boundaries. The singular control arc also results in a constant α_s in the second step for both the models. So the optimal input is a piece-wise constant strategy. The second step derived is a CVD mode for the LF_1 model and a VVD mode for the GLF model. As we can see the numerical values of α_s are similar for both the models.

3.1 Case study

The experiment objective was to drive the lactose concentration from 50 g/L to 110 g/L, and to reduce the NaCl concentration from 5.3 g/L to 1 g/L, using NDF. The initial volume of the solution was 21 L. The three strategies were implemented, i.e.

(1) traditional ($\alpha = \{0, 1\}$): concentrate using C mode till lactose increases to final concentration ($c_1 = c_{1,\mathrm{f}} = 110\,\mathrm{g/L}$), then using CVD mode reduce NaCl to reach the final objective ($c_2 = c_{2,\mathrm{f}} = 1\,\mathrm{g/L}$).
(2) optimal ($\alpha = \{0, \alpha_s, \infty\}$):
   (a) Use C mode to drive from initial concentrations to reach singular surface ($S = 0$), for both GLF and LF_1 models; i.e. concentrate till lactose concentration (c_1) is 332.7 g/L for GLF, and $\gamma_2/\mathrm{e} = 458.6\,\mathrm{g/L}$ in case of LF_1.

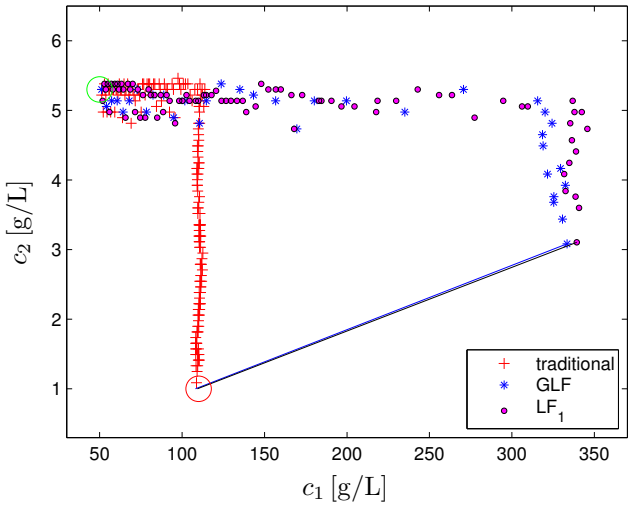

Fig. 5. Concentration measurements of lactose and NaCl for traditional and optimal strategies, along with the initial and final conditions.

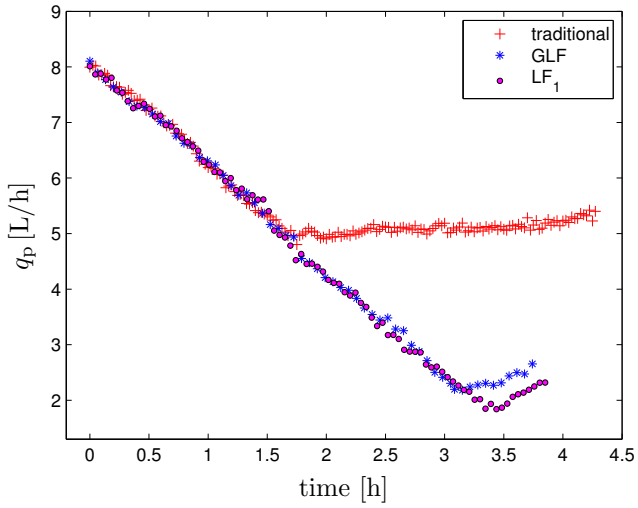

Fig. 6. Permeate flow rate measurements of traditional and optimal strategies.

(b) Stay on the singular surface using singular control α_s, till the condition $c_1/c_2 = c_{1,\mathrm{f}}/c_{2,\mathrm{f}}$ is met. The separation process ends with this step.

(c) The final step is to get the final concentrations using D mode, and it practically takes negligible amount of time. This is represented by the continuous line to the final concentrations (red circle) in Fig. 5.

The volume measurement device on the plant is constrained by 3-32 L. As we use volume measurement to get the concentration of lactose (5), hence for the given initial volume of 21 L, the maximum concentration of lactose is constrained to 340 g/L. The implementation of LF_1 strategy was thus compromised, and instead of concentrating lactose to 458.6 g/L, we concentrated to 340 g/L.

The results and comparison of the three strategies is quantified and represented in Figs. 5 and 6 and Table 2. Figure 5 shows evolution of concentrations $c_1(t)$ and $c_2(t)$, where the initial and final points are marked as green and red circle, respectively. The dilution mode, which is present for optimal strategies derived from GLF and LF_1 model, is represented by solid lines. It is clear that all three strategies were able to drive the solution to the desired concentrations of lactose and NaCl.

Table 2. Comparison of time taken by traditional and optimal strategies.

Strategy	t_1 [h]	t_2 [h]	t_f [h]	Δt_f [%]
traditional	1.75	2.53	4.28	100
GLF	3.08	0.66	3.74	87
LF_1	3.35	0.50	3.85	90

The permeate flow rate diagram (Fig. 6) shows that all strategies started at similar initial flow rate as the initial concentrations were identical. The trend of decrease in flow rate as the concentration of lactose increased is also same for all three of them. The reason behind the reduction of time with time-optimal strategy (Table 2) is the step when NaCl concentration is reduced. It can be observed in the flow rate figure that although due to over-concentrating lactose in optimal strategies the C mode takes longer time (t_1 in Table 2), as a result the time for CVD in case of LF_1 and VVD in case of GLF reduces (t_2 in Table 2). This reduction results in overall reduction of time (t_f in Table 2) as we stop the process after CVD/VVD, and do the instantaneous D mode to reach the desired concentrations. The optimal strategies took 87-90 % of the time taken by traditional strategy (Δt_f in Table 2).

Besides minimizing time, this analytically derived optimal strategy holds the benefit, i.e. no extra hardware needs to be installed on the existing plant. No on-line calculations/optimizations are required: the switching concentrations and control need to be found out prior to the start of experiment.

The models fitted were good enough but were still not perfect, in context of time-optimal operation. As we can see from the equation for S (12), that during the VVD mode the permeate flow rate should be constant, i.e. $q_\mathrm{p} = \gamma_1 (\gamma_3 + 1)$. Now, if we look at the experimental values of q_p from Fig. 6, we observe that during the VVD mode for optimal GLF operation the permeate flow is varying. This may result from the differences in model parameters from one batch to another, and because the optimal switchings were done based on concentration and not on q_p. This could be avoided by estimating the model while performing the experiment (online parameter estimation). This may result in implementation of a truly real-time time-optimal strategy, but on the expense of online calculations/estimations.

4. CONCLUSION

We have presented a control strategy for the time-optimal operation of diafiltration processes in order to concentrate lactose and reduce the concentration of NaCl. Based on the experiments with lactose and NaCl, parameters of two permeate flux models were estimated. The first model being a function of both lactose and NaCl concentrations (generalized limiting flux), while second one as a function of only lactose concentration (limiting flux). Based on the fitted models, a time-optimal control problem was formu-

lated. The solution was found by employing the analytical solution from our earlier work, using Pontryagin's minimum principle. The presented approach was then tested on a case study. The optimal and the traditional industrial strategies were implemented on a pilot scale membrane separation unit. The time-optimal strategies were found to consist of three steps, i.e. bang-bang on the boundaries and singular control in the middle step. The performance of the time-optimal strategies was compared with traditional two-step operational strategy. The quantitative results show that the proposed approach is successful and at least 10% faster than traditional industrial strategy to reach the desired concentrations. The future step would be to study and experiment on cases with different initial conditions such that the analytical singular surface for limiting flux optimal strategy is attainable.

ACKNOWLEDGEMENTS

We gratefully acknowledge the contribution of the Slovak Research and Development Agency (project APVV-15-0007) and the Scientific Grant Agency of the Slovak Republic (project 1/0004/17).

REFERENCES

Artuğ, G. (2007). *Modelling and Simulation of Nanofiltration Membranes*. Cuvillier.

Blatt, W., Dravid, A., Michaels, A., and Nelsen, L. (1970). Solute polarization and cake formation in membrane ultrafiltration: Causes, consequences, and control techniques. In *Membrane Science and Technology*, 47–97. Springer US.

Boerefijn, R., Ning, Z., and Ghadiri, M. (1998). Disintegration of weak lactose agglomerates for inhalation applications. *International Journal of Pharmaceutics*, 172(12), 199 – 209.

Chandrapala, J., Duke, M.C., Gray, S.R., Weeks, M., Palmer, M., and Vasiljevic, T. (2016). Nanofiltration and nanodiafiltration of acid whey as a function of ph and temperature. *Separation and Purification Technology*, 160, 18 – 27.

Chen, Z., Luo, J., Wang, Y., Cao, W., Qi, B., and Wan, Y. (2017). A novel membrane-based integrated process for fractionation and reclamation of dairy wastewater. *Chemical Engineering Journal*, 313, 1061 – 1070.

Cohen, J.L., Barile, D., Liu, Y., and de Moura Bell, J.M. (2017). Role of ph in the recovery of bovine milk oligosaccharides from colostrum whey permeate by nanofiltration. *International Dairy Journal*, 66, 68 – 75.

Conidi, C., Cassano, A., Caiazzo, F., and Drioli, E. (2017). Separation and purification of phenolic compounds from pomegranate juice by ultrafiltration and nanofiltration membranes. *Journal of Food Engineering*, 195, 1 – 13.

Das, B., Sarkar, S., Sarkar, A., Bhattacharjee, S., and Bhattacharjee, C. (2016). Recovery of whey proteins and lactose from dairy waste: A step towards green waste management. *Process Safety and Environmental Protection*, 101, 27 – 33.

Fikar, M., Kovács, Z., and Czermak, P. (2010). Dynamic optimization of batch diafiltration processes. *Journal of Membrane Science*, 355(1), 168 – 174.

Foley, G. (2006). Water usage in variable volume diafiltration: comparison with ultrafiltration and constant volume diafiltration. *Desalination*, 196, 160 – 163.

Gutiérrez, L.F., Hamoudi, S., and Belkacemi, K. (2012). Lactobionic acid: A high value-added lactose derivative for food and pharmaceutical applications. *International Dairy Journal*, 26(2), 103 – 111.

Hermia, J. (1982). Constant pressure blocking filtration laws-application to power-law non-Newtonian fluids. *Transactions of the Institution of Chemical Engineers*, 60(2), 183 – 187.

Jaffrin, M. and Charrier, J. (1994). Optimization of ultrafiltration and diafiltration processes for albumin production. *Journal of Membrane Science*, 97, 71 – 81.

Jelemenský, M., Paulen, R., Fikar, M., and Kovács, Z. (2015). Time-optimal operation of multi-component batch diafiltration. *Computers & Chemical Engineering*, 83, 131 – 138.

Lutz, H. (2015). *Ultrafiltration for Bioprocessing*. Woodhead Publishing.

Paulen, R. and Fikar, M. (2016). *Optimal Operation of Batch Membrane Processes*. Springer.

Pontryagin, L.S., Boltyanskii, V.G., Gamkrelidze, R.V., and Mishchenko, E.F. (1962). *The Mathematical Theory of Optimal Processes*. Wiley, New York.

Rajagopalan, N. and Cheryan, M. (1991). Process optimization in ultrafiltration: Flux-time considerations in the purification of macromolecules. *Chemical Engineering Communications*, 106(1), 57–69.

Salehi, F. (2014). Current and future applications for nanofiltration technology in the food processing. *Food and Bioproducts Processing*, 92(2), 161 – 177.

Sharma, A., Jelemenský, M., Paulen, R., and Fikar, M. (2016). Estimation of membrane fouling parameters for concentrating lactose using nanofiltration. In *26th European Symposium on Computer Aided Process Engineering*, volume 26, 151–156. Elsevier B.V., Portorož, Slovenia.

Sharma, A., Jelemenský, M., Paulen, R., and Fikar, M. (2017). Optimal operation of nanofilter based diafiltration processes using experimental permeation models. In *Proceedings of the 21st International Conference on Process Control*, 185–190.

Synder (2014). Nanofiltration membrane elements. Synder Sanitory Catalog 2014 - Synder Filtration.

Tang, C.Y. and Leckie, J.O. (2007). Membrane independent limiting flux for RO and NF membranes fouled by humic acid. *Environmental Science & Technology*, 41(13), 4767–4773.

van den Berg, G. and Smolders, C. (1990). Flux decline in ultrafiltration processes. *Desalination*, 77, 101 – 133.

Verasztó, B., Sharma, A., Nguyen, Q.D., Vatai, G., Czermak, P., and Kovács, Z. (2013). Membrane filtration technology for processing whey and converting whey-based lactose into galactooligosaccharides. In J. Krzysztoforski and M. Szwast (eds.), *Conference Proceeding of the 6th Membrane Conference of Visegrad Countries*, E5. Polish Membrane Society, Warsaw, Poland.

Yin, N., Yang, G., Zhong, Z., and Xing, W. (2011). Separation of ammonium salts from coking wastewater with nanofiltration combined with diafiltration. *Desalination*, 268(13), 233 – 237.